

14

Elastic scattering at high energies

Elastic scattering is in some sense the most fundamental type of reaction, but it is also the most difficult to understand theoretically. There is a huge amount of spin-dependent data at low to medium energies, but little understanding of the mechanisms at work. In several instances, however, spin-dependent data have played a crucial rôle in nailing the coffin of a current theoretical picture. Somehow, simple-minded ideas, which succeed in explaining gross features of cross-sections, angular distributions etc., run aground when faced with the more probing questions involved in spin-dependent reactions. Because of the lack of clear-cut theoretical ideas and because of the difficulty of the experiments there has generally been a lack of experimental effort in this field since the mid-1980s, but this situation is about to change with the commissioning of the RHIC collider at Brookhaven. There, besides a major programme of heavy-ion physics, it will be possible to study pp collisions, with both beams polarized and up to an energy of 250 GeV per beam. Consequently we shall concentrate in this chapter on nucleon–nucleon scattering.

Broadly speaking there are two kinematic regions of interest, small to medium values of momentum transfer and large momentum transfer. The first is, strictly speaking, in the domain of non-perturbative QCD, so there are no precise theoretical predictions, though there are very interesting suggestive hints. In the second region perturbative QCD ought to be applicable and, indeed, very powerful theoretical results have been derived. It is a well-known secret that there is a major disagreement between present data and these predictions. The usual argument for not therefore abandoning QCD, and it is a sound one, is that the data are not yet at large enough energy and momentum transfer to justify fully a perturbative treatment. With the increased kinematic range at RHIC we will thus be facing some very challenging questions: either the trend of

the experimental results must begin to change or we must seriously begin to question the validity of QCD.

14.1 Small momentum transfer: general

Consider proton–proton elastic scattering with momenta as indicated:

$$p(p_1) + p(p_2) \rightarrow p(p_3) + p(p_4). \quad (14.1.1)$$

There are five independent helicity amplitudes corresponding to the following transitions:

$$\begin{aligned} \phi_1 &= \langle ++ | T | ++ \rangle & \phi_2 &= \langle ++ | T | -- \rangle \\ \phi_3 &= \langle +- | T | +- \rangle & \phi_4 &= \langle +- | T | -+ \rangle \\ \phi_5 &= \langle ++ | T | +- \rangle \end{aligned} \quad (14.1.2)$$

Relations between these and any other helicity amplitude can be determined via the symmetry relations given in Section 4.2. Each of the ϕ_j is a function of the Mandelstam variables

$$s = (p_1 + p_2)^2 \quad t = (p_1 - p_3)^2 \quad u = (p_1 - p_4)^2 \quad (14.1.3)$$

with

$$s + t + u = 4m^2. \quad (14.1.4)$$

In the CM of the reaction, where the protons all have a magnitude of momentum p , one has

$$\begin{aligned} s &= 4E^2 = 4(p^2 + m^2) \\ t &= -2p^2(1 - \cos \theta) \\ u &= -2p^2(1 + \cos \theta) \end{aligned} \quad (14.1.5)$$

where θ is the CM scattering angle.

There is a large number of spin-dependent observables that one can measure. A comprehensive list is given in Table A10.4, and expressions for the observables in terms of the ϕ_j are given in Tables A10.5 and A10.6.

The conservation of angular momentum imposes restrictions on the helicity-flip amplitudes in the forward direction (Section 4.3), namely

$$\phi_5 \propto \sqrt{-t} \quad \phi_4 \propto t \quad (14.1.6)$$

as $t \rightarrow 0$.

In the region of very small t , as discussed in subsection 8.1.1, we have interference between the hadronic and electromagnetic amplitudes and we shall presently explain some new results in this field. Firstly, however, we shall summarize what is known about the hadronic amplitudes near the forward direction. It is convenient to analyse the high energy behaviour

of the ϕ_j in terms of the quantum numbers of the system that can be exchanged between the protons, and the singularities at $J = \alpha(t)$ in the complex angular momentum plane associated with such a system. (For an introduction to the concept of complex angular momentum see Gasiorowicz, 1967, Chapter 28.) In this discussion it will be convenient to use helicity amplitudes normalized such that

$$\frac{d\sigma}{dt} = \frac{2\pi}{s^2} (|\phi_1|^2 + |\phi_2|^2 + |\phi_3|^2 + |\phi_4|^2 + 4|\phi_5|^2). \tag{14.1.7}$$

Then, via the optical theorem,

$$\sigma_{\text{tot}}(s) = \frac{4\pi}{s} \text{Im} [\phi_1(s, t) + \phi_3(s, t)]_{t=0}. \tag{14.1.8}$$

A singularity at $J = \alpha(t)$ then implies an asymptotic behaviour

$$|\phi(s, t)| \propto s^{\alpha(t)} \quad \text{as } s \rightarrow \infty \tag{14.1.9}$$

up to possible logarithmic corrections. In this normalization, the rigorous Froissart–Martin bound (Froissart, 1961; Martin, 1966) reads

$$|\phi_1(s, t) + \phi_3(s, t)|_{t=0} \lesssim \text{constant} \times s \ln^2 s \quad \text{as } s \rightarrow \infty \tag{14.1.10}$$

or

$$\sigma_{\text{tot}} \lesssim \text{constant} \times \ln^2 s \quad \text{as } s \rightarrow \infty \tag{14.1.11}$$

so that the leading J -plane singularity cannot lie above $J = 1$ at $t = 0$.

A particular dynamical exchange mechanism is classified according to its quantum numbers: *parity* (\mathcal{P}), *charge conjugation* (\mathcal{C}) and *signature* (τ). An amplitude is called *even* or *odd* under *crossing*, i.e. under the analytic continuation

$$s \rightarrow e^{i\pi} s \tag{14.1.12}$$

for $\tau = \pm 1$, since

$$A_\tau(e^{i\pi} s, t) = \tau A_\tau^*(s, t). \tag{14.1.13}$$

For nucleon–nucleon scattering there are three classes of exchange (Leader and Slansky, 1966), as indicated in Table 14.1, which also shows to which

Table 14.1. Classification of exchanges and the amplitudes to which they contribute to in pp scattering

	Class 1 $\tau = \mathcal{P} = \mathcal{C}$	Class 2 $\tau = -\mathcal{P} = -\mathcal{C}$	Class 3 $\tau = -\mathcal{P} = \mathcal{C}$
amplitudes	$\phi_1 + \phi_3, \phi_5, \phi_2 - \phi_4$	$\phi_1 - \phi_3$	$\phi_2 + \phi_4$
particles or mechanism	$P, O, \rho, \omega, f, a_2$	a_1	π, η, b

amplitudes, or combination of amplitudes, each class contributes. Also shown in Table 14.1 are some particles whose quantum numbers coincide with each class. P, the *pomeron* and O, the *odderon* are not particles, but label dynamical systems with the quantum numbers of the vacuum, $\mathcal{P} = +1, \mathcal{C} = +1, \tau = +1$ (the pomeron), or $\mathcal{P} = +1, \mathcal{C} = -1, \tau = -1$ (the odderon).

The pomeron is important because if one single exchange mechanism dominates at asymptotic energies, it has to have the quantum numbers of the vacuum (Peierls and Trueman, 1964).

The singularities associated with the other particles in Table 14.1 all lie well below $J = 1$ and the pomeron is supposed to have a singularity at $J = 1$ when $t = 0$ in order to explain the fact that both σ_{pp} and $\sigma_{\bar{p}p}$ appear to be growing like $\ln^2 s$ at the highest energies measured.

The rôle of the odderon is interesting, because it is the quantum number \mathcal{C} that determines the relative sign of the contribution of a given exchange system to $pp \rightarrow pp$ and $\bar{p}p \rightarrow \bar{p}p$:

$$A_{\tau, \mathcal{P}, \mathcal{C}}^{\bar{p}p}(s, t) = \mathcal{C} A_{\tau, \mathcal{P}, \mathcal{C}}^{pp}(s, t). \tag{14.1.14}$$

It was believed for decades that asymptotically one had to have

$$A^{\bar{p}p} - A^{pp} \rightarrow 0 \quad \text{as } s \rightarrow \infty \tag{14.1.15}$$

but Łukaszuk and Nicolescu (1973) pointed out that in fact

$$A^{\bar{p}p} - A^{pp} \not\rightarrow 0 \quad \text{as } s \rightarrow \infty \tag{14.1.16}$$

is compatible with all known general properties of field theory. The odderon is the name given to the putative mechanism responsible for this (Joynson, Leader and Nicolescu, 1975).

If for example one has

$$A^{pp} = A_P + A_O \tag{14.1.17}$$

then

$$A^{\bar{p}p} = A_P - A_O \tag{14.1.18}$$

and the analysis of Łukaszuk and Nicolescu showed that it was possible to have

$$\frac{|A_O|}{|A_P|} \not\rightarrow 0 \quad \text{as } s \rightarrow \infty. \tag{14.1.19}$$

The pomeron and odderon mechanisms are believed to reflect two-gluon and three-gluon exchange in QCD. Although it is not possible to carry out a QCD calculation in the truly soft, non-perturbative, regime, powerful conformal field-theoretic methods have been utilized by Lipatov and co-workers (Lipatov, 1986; 1989; Braun, Gauron and Nicolescu, 1999)

to study fully interacting two- and three-gluon exchange dynamics just outside the soft region. The two-gluon dynamics leads to a system with a singularity just above $J = 1$ (often called the QCD pomeron), and the three-gluon case to a singularity with $\mathcal{C} = -1$ just below but very close to $J = 1$, which is identified with the odderon.

There is no convincing experimental evidence for the odderon though there are hints of a difference between $d\sigma/dt$ for pp and $\bar{p}p$ at small t in the ISR data at $\sqrt{s} = 53$ GeV. But all in all the data on total cross-sections and on the ratio of real to imaginary parts of forward spin-averaged amplitudes suggest that the coupling of the odderon to $\phi_1 + \phi_3$ at $t = 0$ is much smaller than that of the pomeron:

$$\frac{|\phi_1 + \phi_3|_O}{|\phi_1 + \phi_3|_P} \lesssim 2\%. \quad (14.1.20)$$

On the one hand, almost nothing is known about the coupling of P or O to the other helicity amplitudes, though Hinotani, Neal, Predazzi and Walters (1979) claimed some evidence for a roughly energy-independent single-helicity-flip amplitude. For a more modern assessment see Buttimore *et al.* (1999).

On the other hand we do have some knowledge about the phases of the amplitudes. Because of the analytic properties of the scattering amplitude in the complex s -plane the phase of an amplitude, in the asymptotic regime, is governed by its energy dependence and its signature τ (Eden, 1971). If the asymptotic behaviour due to an exchange system with signature τ is

$$|A_\tau| \approx s^\alpha (\ln s)^p \quad \text{as } s \rightarrow \infty \quad (14.1.21)$$

then one has for $\tau = +1$

$$A_+ \approx s^\alpha (\ln s)^p e^{-i\pi\alpha/2} \left(1 - \frac{i\pi p}{2 \ln s}\right), \quad (14.1.22)$$

whereas, for $\tau = -1$, the behaviour is

$$A_- \approx i s^\alpha (\ln s)^p e^{-i\pi\alpha/2} \left(1 - \frac{i\pi p}{2 \ln s}\right). \quad (14.1.23)$$

Measurements of spin-dependent observables often have helped and will continue to help to disentangle the dynamical effects.

A case in point is Regge pole theory. Many aspects of the behaviour of the small- t differential cross-sections, their shrinkage etc., in a wide range of reactions were well described by Regge pole exchange. There was even some success with polarizations since the Regge pole exchange amplitudes are not real and possess a natural phase needed to obtain non-zero polarization (see Table A10.5). But in $\pi^-p \rightarrow \pi^0n$ only one Regge pole can be exchanged, the ρ , so that both helicity-flip and non-flip

amplitudes have the same phase and the polarization vanishes (see Table A10.1). Nonetheless, significant polarizations were measured.

Another aspect of Regge pole theory that runs counter to spin-dependent results is the property of factorization (Fox and Leader, 1967). In $pp \rightarrow pp$, for example, one has

$$\langle \lambda'_1, \lambda'_2 | T | \lambda_1, \lambda_2 \rangle^{\text{R.pole}} \propto \beta_{\lambda'_1 \lambda_1}(t) \beta_{\lambda'_2 \lambda_2}(t) s^{\alpha(t)} \tag{14.1.24}$$

where the $\beta(t)$ are called *residue functions*.

This, via (14.1.2), leads to

$$\phi_2 = \phi_5^2 / \phi_1 \tag{14.1.25}$$

so that, from (14.1.6)

$$\phi_2^{\text{R.pole}} \propto t \quad \text{as } t \rightarrow 0. \tag{14.1.26}$$

(A comprehensive account of the spin properties of Regge poles is given in Leader (1969).)

The vanishing of ϕ_2 at $t = 0$ would be a totally dynamic effect, but it and similar predictions do not seem to agree with the data, though it must be said that there is a real scarcity of data at really high energies.

For instance, the transverse cross-section difference $\Delta\sigma_T$ defined in (5.1.12) is proportional to $\text{Im } \phi_2$ at $t = 0$. It is certainly not zero in the low to medium energy region, but the rather limited data do suggest that

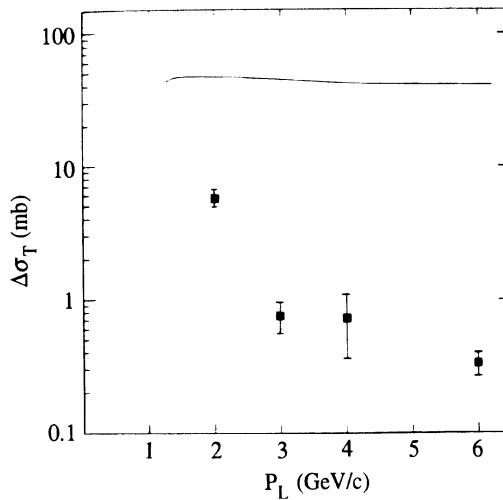


Fig. 14.1 The transverse cross-section difference $\Delta\sigma_T$ for $pp \rightarrow pp$. The line in the upper part of the graph gives σ_{tot} (spin ave.). (From de Boer *et al.*, 1975.)

it is decreasing rapidly with energy (see Fig. 14.1.) Another case is the longitudinal cross-section difference $\Delta\sigma_L$ in (5.1.11): it is proportional to $\text{Im}(\phi_1 - \phi_3)$ at $t = 0$. But factorization (14.1.24) together with a parity property of the contribution of a single Regge pole to the $pp \rightarrow pp$ helicity amplitudes,

$$\langle \lambda'_1; -\lambda'_2 | T | \lambda_1; -\lambda_2 \rangle = \tau \mathcal{P} \langle \lambda'_1; \lambda'_2 | T | \lambda_1; \lambda_2 \rangle, \quad (14.1.27)$$

leads to $\phi_1 = \phi_3$ for the dominant poles, which all have $\tau \mathcal{P} = +1$. Hence one would expect $\Delta\sigma_L$ to decrease with energy.

As seen in Fig. 14.2, $\Delta\sigma_L$ has a complicated structure at low-to-medium energies but is decreasing in magnitude fast with energy.

From our present-day perspective, we prefer to think of a Regge exchange contribution as something more complex than a pole, perhaps a so-called *cut* or a pole–cut combination, with a characteristic energy dependence and phase but without the factorization property of its couplings. The decrease of $\Delta\sigma_L$ with energy is then quite compatible with its being controlled by an exchange system with the quantum numbers of the a_1 (see Table 14.1), which is expected to have an effective $\alpha(0) \approx 1/2$.

The behaviour of $\Delta\sigma_T$ is more interesting, since in principle it could receive contributions from both the pomeron and odderon, leading to its growing at higher energies. This will be studied at the RHIC collider and will provide important information about the spin couplings of pomeron and odderon. (A detailed analysis can be found in Leader and Trueman, 2000.)

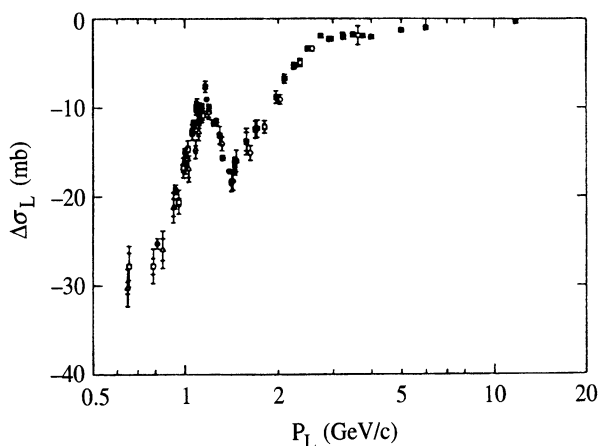


Fig. 14.2 Longitudinal cross-section difference $\Delta\sigma_L$ for $pp \rightarrow pp$. (From Grosnick *et al.*, 1997.)

It turns out that the study of spin dependence is greatly facilitated by studying the Coulomb interference region, where the interference between the hadronic amplitudes and the *known* electromagnetic amplitude helps in the process of identifying the details of the hadron dynamics.

14.2 Electromagnetic interference revisited

We shall now explain the newly discovered fact (Buttimore *et al.*, 1999) that *pp* elastic scattering is *self-calibrating*, in the sense that a sufficient number of measurements of spin-dependent observables at very small t , in the Coulomb interference region, allows one not only to determine most of the helicity amplitudes but also the polarization of the beam and target.

It will be seen that the method involves the taking of several ratios of possibly very small quantities, so that the precision needed may be difficult to achieve experimentally. However, so little is known about the amplitudes at high energy that we are unable to quantify this matter. We shall follow the treatment of Buttimore *et al.* (1999).

At the very small values of t in which we are interested, the interference between the strong and electromagnetic forces can be taken into account by writing

$$\phi_j = \phi_j^N e^{-i\delta} + \phi_j^{\text{EM}} \quad (14.2.1)$$

where the ϕ_j^{EM} are the one-photon exchange amplitudes given in (8.1.5), multiplied by $s/(2\sqrt{\pi})$. The Coulomb phase δ was shown by Buttimore, Gotsman and Leader (1978) to be the same for all helicity amplitudes. It is very small and we shall ignore it in our approximate treatment.

We assume the beam has polarization P and the target P' . In a *pp* collider it will be true to an extremely high degree of accuracy that $P = \pm P'$, depending on the machine setting. We consider the experimentally measured asymmetries, which are given by $PA d\sigma/dt$, $PP' A_{NN} d\sigma/dt$ etc. These contain singular terms at $t \rightarrow 0$ coming from interference between the one-photon and the hadronic amplitudes. To order α the asymmetries involving A_{NN} , A_{SS} and A_{LL} are singular like $1/t$ whereas A and A_{SL} go like $1/\sqrt{-t}$.¹ From the work of Buttimore, Gotsman and Leader (1978) we can write, for very small t ,

$$-\frac{m\sqrt{-t}}{\sigma_{\text{tot}}} PA \frac{d\sigma}{dt} = \alpha a_N + \frac{\sigma_{\text{tot}}}{8\pi} b_N t + \dots \quad (14.2.2)$$

$$\frac{t}{\sigma_{\text{tot}}} PP' A_{LL} \frac{d\sigma}{dt} = \alpha a_{LL} + \frac{\sigma_{\text{tot}}}{8\pi} b_{LL} t + \dots \quad (14.2.3)$$

¹ The connection between these asymmetry parameters and the CM parameters is given in Table A10.7, and the relation to the helicity amplitudes then follows via Table 10.5. Note that here A stands for $A_{\text{ARG}}^{(A)}$.

$$\frac{t}{\sigma_{\text{tot}}} PP' A_{NN} \frac{d\sigma}{dt} = \alpha a_{NN} + \frac{\sigma_{\text{tot}}}{8\pi} b_{NN} t + \dots \tag{14.2.4}$$

$$\frac{t}{\sigma_{\text{tot}}} PP' A_{SS} \frac{d\sigma}{dt} = \alpha a_{SS} + \frac{\sigma_{\text{tot}}}{8\pi} b_{SS} t + \dots \tag{14.2.5}$$

$$-\frac{m\sqrt{-t}}{\sigma_{\text{tot}}} PP' A_{SL} \frac{d\sigma}{dt} = \alpha a_{SL} + \frac{\sigma_{\text{tot}}}{8\pi} b_{SL} t + \dots \tag{14.2.6}$$

Expressions for the a_j and b_j are given in Table 14.2 in terms of the following rescaled amplitudes, which may be taken independent of t :

$$R_2 + iI_2 = \frac{\phi_2^N(s, t)}{2 \text{Im } \phi_+^N(s)} \tag{14.2.7}$$

$$R_- + iI_- = \frac{\phi_-^N(s, t)}{\text{Im } \phi_+^N(s)} \tag{14.2.8}$$

$$R_5 + iI_5 = \left(\frac{m}{\sqrt{-t}} \right) \frac{\phi_5^N(s, t)}{\text{Im } \phi_+^N(s)} \tag{14.2.9}$$

where

$$\phi_{\pm}^N(s, t) = \frac{1}{2} \left[\phi_1^N(s, t) \pm \phi_3^N(s, t) \right] \tag{14.2.10}$$

and

$$\text{Im } \phi_+^N(s) \equiv \text{Im } \phi_+^N(s, t = 0) = \frac{s}{8\pi} \sigma_{\text{tot}}, \tag{14.2.11}$$

the latter via the optical theorem. Also, as usual,

$$\rho = \frac{\text{Re } \phi_+^N(s, 0)}{\text{Im } \phi_+^N(s, 0)}. \tag{14.2.12}$$

In Table 14.2, terms of order αt are omitted. In this approximation $A_{NN} = A_{SS}$ and measurement of these quantities could be used as a check on the validity of the approximations. Indeed, the entire procedure can

Table 14.2. Expressions for the coefficients a_j and b_j in eqns (14.2.2) to (14.2.6). κ is the anomalous magnetic moment of the proton

Observable	a_j	b_j
A_{NN}	$PP'R_2$	$PP'[R_2(\rho + R_-) + I_2(1 + I_-)]$
A_{LL}	$PP'R_-$	$PP'[\rho R_- + I_- + R_2^2 + I_2^2]$
A_{SL}	$PP'\frac{\kappa}{2}(R_2 + R_-)$	$PP'[R_5(R_2 + R_-) + I_5(I_2 + I_-)]$
A	$P[I_5 - \frac{\kappa}{2}(1 + I_2)]$	$P[I_5(\rho + R_2) - R_5(1 + I_2)]$

be tested by checking whether the measured quantities in (14.2.2)–(14.2.6) are linear functions of t .

In addition to the above observables we need to know the cross-section differences $\Delta\sigma_L$ and $\Delta\sigma_T$ defined in (5.1.11) and (5.1.12). The measured observables we use are

$$\delta_T \equiv -\frac{1}{2}PP' \frac{\Delta\sigma_T}{\sigma_{\text{tot}}} = PP'I_2 \quad (14.2.13)$$

and

$$\delta_L \equiv \frac{1}{2}PP' \frac{\Delta\sigma_L}{\sigma_{\text{tot}}} = PP'I_- \quad (14.2.14)$$

Having measured ρ , a_{NN} , a_{LL} , δ_L and δ_T we can substitute in the expression for b_{LL} to obtain

$$b_{LL} = \rho a_{LL} + \delta_L + \frac{a_{NN}^2 + \delta_T^2}{PP'} \quad (14.2.15)$$

from which one obtains an expression for the polarization,

$$PP' = \frac{a_{NN}^2 + \delta_T^2}{b_{LL} - \rho a_{LL} - \delta_L}, \quad (14.2.16)$$

whence, since it will be known whether $P' = P$ or $P' = -P$, one can obtain P . The sign ambiguity should be innocuous.

Knowing PP' one can now obtain the values of R_2 , I_2 , R_- , I_- from a_{NN} , δ_T , a_{LL} and δ_L respectively.

In practice, it may turn out that the errors on PP' obtained from (14.2.16) are unacceptably large. In that case there is an alternative procedure, which should be more accurate.

The analysing power of the reaction is given by

$$\begin{aligned} \frac{m\sqrt{-t}}{\sigma_{\text{tot}}} A \frac{d\sigma}{dt} &= \left(\frac{\kappa}{2} - I_5 + \frac{\kappa}{2} I_2 \right) \\ &+ \frac{\sigma_{\text{tot}}}{8\pi} [R_5(1 + I_2) - I_5(\rho + R_2)] t \end{aligned} \quad (14.2.17)$$

and this is expected to be very largely dominated by the term $\kappa/2$. Thus the other terms in (14.2.17) are small corrections and large errors on them may be unimportant. We already have values for ρ , R_2 and I_2 . There is a lengthy algebraic procedure for estimating R_5 and I_5 from the measurement of a_{SL} , b_{SL} , a_N and b_N and which uses (14.2.16). One finds

$$I_5 = \frac{\kappa}{2} \left(\frac{b_{SL}}{a_{SL}} - \frac{b_N}{a_N} \right) / \left(\frac{\delta_T + \delta_L}{a_{NN} + a_{LL}} - \frac{b_N/a_N - \rho - a_{NN}O_1}{1 + \delta_T O_1} \right) \quad (14.2.18)$$

$$R_5 = \frac{\kappa b_{SL}}{2 a_{SL}} - \frac{\delta_T + \delta_L}{a_{NN} + a_{LL}} I_5 \quad (14.2.19)$$

where O_1 is the estimate for PP' given in (14.2.16).

Using these should provide a relatively accurate estimate of the analysing power, after which the reaction can be used directly to measure the proton polarization.

A more accurate treatment of the problem, including a discussion of the rôle of the Coulomb phase, can be found in Buttimore, Leader and Trueman (1999).

It turns out that the measurement of spin-dependent observables in the interference region could also be helpful in trying to understand the rôle of the odderon; in particular A_{NN} is sensitive to it. A detailed discussion of this issue is given in Leader and Trueman (2000).

14.3 Elastic scattering at large momentum transfer

Considered as a QCD reaction, elastic proton–proton scattering is manifestly a very complex process. Even in its simplest version, taking into account only the valence quarks, one has to deal with a six-quark \rightarrow six-quark reaction. Examples of Feynman diagrams for such an interaction are shown in Fig. 14.3 (the Brodsky–Lepage hard-scattering mechanism)

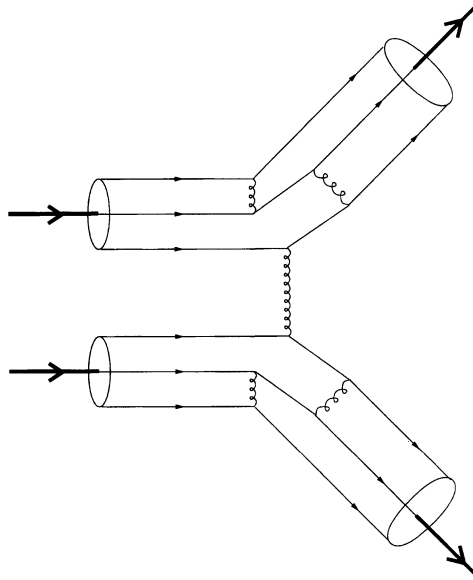


Fig. 14.3 A Brodsky–Lepage diagram for large-momentum-transfer $pp \rightarrow pp$ (Brodsky and Lepage, 1980).

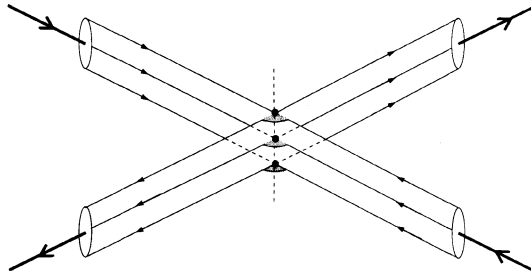


Fig. 14.4 A Landshoff diagram for large-momentum-transfer $pp \rightarrow pp$ (Landshoff, 1974.)

and in Fig. 14.4 (the Landshoff mechanism). Despite the complexity it turns out that one can deduce powerful results for the spin dependence in the asymptotic limit where $|s|$ and $|t|$ are $\gg m^2$. The problem, as will become clear, is precisely where one can expect the asymptotic behaviour to set in. It will be seen that the present experimental data badly contradict these asymptotic predictions but that there are theoretical arguments, indicating many subtle effects, which suggest that the present-day experiments are still far from the asymptotic regime. However, while these effects alter the momentum-transfer dependence, it is far from clear whether they affect the spin dependence significantly. Hopefully the RHIC collider, if it can probe large enough momentum transfer, will help to resolve the matter.

14.3.1 The asymptotic behaviour

For an exclusive reaction we need the actual wave function of the quarks that make up a hadron. That is, we require to know the amplitude, shown in Fig. 14.5, for the hadron, momentum \mathbf{P} , helicity λ to break up into quarks of momentum \mathbf{q}_j and helicity λ_j . We are considering only reactions with large p_T .

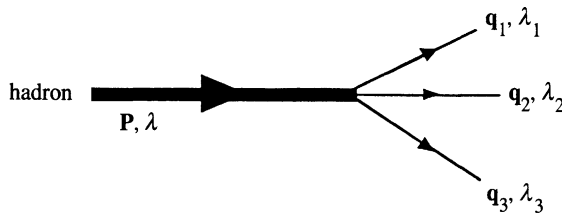


Fig. 14.5. Wave function for three quarks in a hadron.

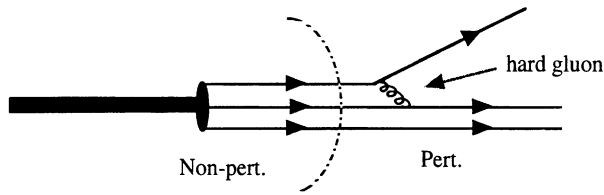


Fig. 14.6. Mechanism for generating a quark with large transverse momentum.

It is believed that the most efficient way to produce large p_T is for each hadron to produce a beam of essentially parallel quarks, which then get a high- p_T kick via a perturbative QCD interaction, shown in Fig. 14.6. So, roughly speaking, the only non-perturbative input is the *soft* amplitude, or wave function, where \mathbf{P} and each \mathbf{q}_j are essentially parallel, say along OZ as shown in Fig. 14.7. Although we cannot compute this soft amplitude we can deduce an important piece of information, as follows. Since all momenta are along OZ any orbital angular momentum must be perpendicular to OZ . Thus the only angular momentum along OZ is spin angular momentum. Conservation of J_z then implies

$$\lambda = \lambda_1 + \lambda_2 + \lambda_3 \tag{14.3.1}$$

for each hadron in the reaction.

Since each quark that interacts perturbatively conserves its helicity (see Section 10.4) we end up with a remarkable result, due to Brodsky and Lepage (1980): in any exclusive reaction

$$A + B \rightarrow C + D + E + \dots$$

one has

$$\lambda_A + \lambda_B = \lambda_C + \lambda_D + \lambda_E + \dots, \tag{14.3.2}$$

that is, *total* initial helicity equals *total* final helicity.

More precisely, what plays the rôle of the soft wave function is the *distribution amplitude*

$$\phi(x, Q^2) = \int_0^{Q^2} d^2\mathbf{k}_T \psi(x, \mathbf{k}_T), \tag{14.3.3}$$

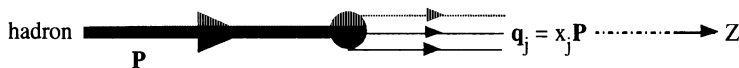


Fig. 14.7 Soft wave function with all quarks essentially parallel to the parent hadron.

i.e. the wave function integrated over a region of the transverse components of the quark momenta. Although the quarks are not strictly parallel to the hadron in this, the integral over \mathbf{k}_T has the effect of eliminating any part of the wave function having $L_z \neq 0$. Thus (14.3.1) and (14.3.2) continue to hold.

Consequences abound! Perhaps the most dramatic example is that the analysing power A in $pp \rightarrow pp$ should vanish because it is proportional to the single-flip helicity amplitude ϕ_5 :

$$A \frac{d\sigma}{dt} = - \text{Im} [\phi_5^*(\phi_1 + \phi_3 + \phi_2 - \phi_4)]. \tag{14.3.4}$$

The vanishing of A follows since ϕ_5 corresponds to the transition

$$|1/2, 1/2\rangle \rightarrow |1/2, -1/2\rangle$$

so that the initial total helicity (= 1) is not equal to the final total helicity (= 0).

Quite contrary to this prediction the analysing power in elastic pp scattering is large all the way out to $p_T^2 \approx 8 \text{ (GeV}/c)^2$. The results of experiments at CERN (Antille *et al.*, 1981) and at the Brookhaven AGS (Crabb *et al.*, 1990) can be seen in Fig. 14.8. (Recall that for $pp \rightarrow pp$ the analysing power A is the same as the polarizing power P .)

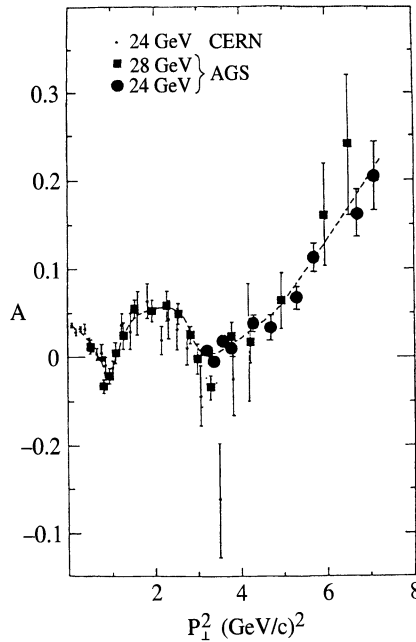


Fig. 14.8. Analysing power for $pp \rightarrow pp$. (From Crabb *et al.*, 1990.)

This contradiction between theory and experiment is usually glossed over by claiming that p_T is too small to expect the asymptotic predictions to hold. This may well be correct, though many papers have pointed out that other ‘asymptotic’ predictions, in inclusive and semi-inclusive reactions, seem to work at precociously low scales, 1–2 (GeV/c)². In fact, as we shall briefly explain, the asymptotic behaviour in exclusive reactions *should* be expected to be less precocious, but if the trend in A shown in Fig. 14.8 continues to much larger values of p_T^2 we will seriously have to question whether our QCD picture of the strong interactions is really correct.

14.3.2 Complications of exclusive reactions

The proton–proton amplitude is immensely complicated: there are some 100 000 Feynman diagrams of the Brodsky–Lepage type. Hence most analyses of the relevance of the asymptotic description have focussed on the much simpler question of electromagnetic form factors at large momentum transfer. A very clear discussion can be found in Kroll (1994) and Jakob and Kroll (1993), whose treatment we follow.

Consider, for simplicity, the pion electromagnetic form factor $F_\pi(Q^2)$. The asymptotic behaviour, as $Q^2 \rightarrow \infty$, is supposed to be controlled by the Feynman diagram in Fig. 14.9, where T_H is the hard scattering amplitude shown in Fig. 14.10 and the hadron \rightarrow quark, antiquark vertices are soft wave functions analogous to those in Fig. 14.7. This leads, in its simplest form, to the remarkable result (Brodsky and Lepage, 1980)

$$Q^2 F_\pi(Q^2) \xrightarrow{Q^2 \rightarrow \infty} 8\pi\alpha_s f_\pi^2 \quad (14.3.5)$$

where $f_\pi = 133$ MeV.

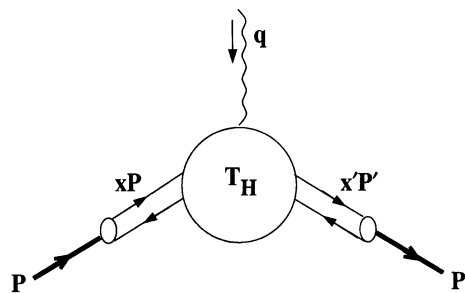


Fig. 14.9. Hard-scattering diagram for pion form factor.

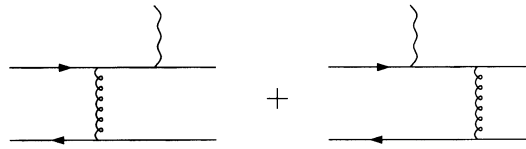


Fig. 14.10. Lowest-order Feynman diagrams for T_H , Fig. 14.9.

A major criticism of this approach was put forward by Isgur and Llewellyn-Smith (1989). Firstly, they showed that in the asymptotic calculation a very large fraction of the result was actually generated from a kinematic region that is not perturbative. The point is that the gluon virtuality in T_H is of order $xx'Q^2$, not Q^2 , so that, for part of the range of integration x and x' are small, we are in a region of small virtuality and a perturbative treatment cannot be justified. *A priori* this is not surprising. What is a shock is the magnitude of the inconsistency. For example, for $F_\pi(Q^2)$ at $Q^2 = 4 (\text{GeV}/c)^2$ only 13% of the result comes from a region where the gluon virtuality is $> 1 (\text{GeV}/c)^2$.

Secondly, Isgur and Llewellyn-Smith pointed out that the contribution from the overlap of initial and final soft wave functions (see Fig. 14.11), given a reasonably gaussian k_T -dependence corresponding to a hadron radius of order 1 fm, is much larger than the asymptotic result (14.3.5). The reason is that even if the k_T -dependence of the wave function cuts off like a gaussian, the overlap only decreases as an inverse power of Q , the precise behaviour depending on the x -dependence of the wave function.

Their astounding conclusion was an estimate that for $\pi N \rightarrow \pi N$ the asymptotic behaviour would only set in for $p_T^2 \geq 10^8 (\text{GeV}/c)^2$!

This, however, is not the end of the story.

In a series of groundbreaking papers Stermann and collaborators (Botts and Stermann, 1989; Li and Stermann, 1992; Li, 1993) demonstrated that it is important to take into account the transverse momentum dependence in T_H (neglected in deriving (14.3.5)) and at the same time to include

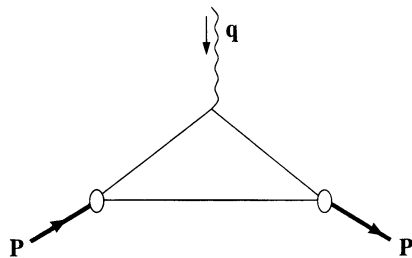


Fig. 14.11. Wave function overlap contribution to the pion form factor.

the effects of so-called Sudakov suppression (Sudakov, 1956), which we shall explain presently. This has a major effect, on the one hand largely negating the Isgur and Llewellyn-Smith criticisms, on the other hand making the treatment of elastic scattering vastly more complicated than in the asymptotic approach.

To understand the physics of Sudakov suppression, recall that in classical electrodynamics the scattering amplitude for non-forward $e + e \rightarrow e + e$ is exactly zero. The reason is that an accelerated electron always radiates photons, so the pure process $ee \rightarrow ee$ cannot occur.

The field-theoretic analogue is that $e + e \rightarrow e + e$ is highly suppressed at large momentum transfer by a ‘Sudakov double logarithm’. For example, for the electromagnetic form factor of an electron at large Q^2 the suppression in the amplitude is (Sudakov, 1956)

$$\exp \left\{ -\frac{e^2}{2\pi} \left[\ln \left(\frac{Q^2}{m_e^2} \right) \right]^2 \right\}, \quad (14.3.6)$$

which goes to zero faster than any inverse power of Q .

Because of the running coupling in QCD, the analogous suppression for the elastic form factor of a quark gets softened to (Mueller, 1981; Sen, 1983)

$$\exp \left\{ \frac{-4C_F}{11 - (2/3)n_f} \ln \left(\frac{Q^2}{\lambda^2} \right) \ln \ln \left(\frac{Q^2}{\lambda^2} \right) \right\} \quad (14.3.7)$$

where λ is an infrared cut-off, and $C_F = 4/3$ for QCD.

In the electron case the probability of emission of a *finite* number of photons in total is also highly suppressed, but the probability to emit any number of photons within some specified energy range is less suppressed, and is the quantity that would be relevant, given the finite energy resolution of any electron detector. But, in the case of the elastic form factor of a hadron the scattered quarks cannot radiate gluons, since in the final state they have to combine to produce the lowest Fock state of the hadron. At first sight, therefore, it seems that the full suppression (14.3.7) should apply.

However, just as an electrically neutral point particle does not suffer the suppression (14.3.6) so a colour-neutral point-like object will not be suppressed by (14.3.7). Hadrons are, of course, colour neutral, but they are extended objects, not point-like. It is then intuitively clear what to expect. For small separations of the constituents, i.e. in the region where perturbative QCD is reliable, there will be little suppression, whereas in the non-perturbative region of large separations the Sudakov factor will drastically suppress the contribution.

The relevant separation turns out to be in a direction perpendicular to the hadron momentum, so one introduces the b -space transform of the wave function,

$$\hat{\psi}(x, \mathbf{b}) = \frac{1}{(2\pi)^2} \int d^2\mathbf{k}_T e^{-i\mathbf{b}\cdot\mathbf{k}_T} \psi(x, \mathbf{k}_T), \quad (14.3.8)$$

and the dominant term in the Sudakov suppression factor then takes the form

$$\exp \left\{ -\frac{2}{3\beta_1} \ln \left(\frac{xQ}{\sqrt{2}\Lambda_{\text{QCD}}} \right) \left[\ln \ln \left(\frac{xQ}{\sqrt{2}\Lambda_{\text{QCD}}} \right) - \ln \ln \left(\frac{1}{b\Lambda_{\text{QCD}}} \right) \right] \right\} \quad (14.3.9)$$

for $b \leq 1/\Lambda_{\text{QCD}}$, where $\beta_1 = (33 - 2n_f)/12$.

The expression in (14.3.9) decreases to zero as b grows from zero to $1/\Lambda_{\text{QCD}}$ and is taken as equal to zero for $b > 1/\Lambda_{\text{QCD}}$. Thus the non-perturbative region of large b is damped out. Moreover it can be shown that the scale to use in $\alpha_s(\mu^2)$ in T_H is not $\mu^2 = xx'Q^2$ but, rather, $\max \{ xx'Q^2, 1/b^2 \}$, so that α_s remains perturbatively small in the calculation.

The net result is that the perturbative calculation, of course vastly more complicated now, should be trustworthy for $Q^2 \gtrsim 4 (\text{GeV}/c)^2$.

Analogous considerations apply to elastic scattering at large momentum transfer, usually expressed in terms of scattering at fixed angle θ in the CM.

The naive perturbative treatment of the Brodsky–Lepage diagrams leads to cross-sections that obey the *dimensional counting-rules* (ignoring logarithms)

$$\frac{d\sigma}{dt}(AB \rightarrow CD) = \left[\frac{\alpha_s(p_T^2)}{s} \right]^{n-2} f(\theta) \quad (14.3.10)$$

where n is the total number of partons in the lowest Fock states of all the particles. Thus for $\pi N \rightarrow \pi N$ we have $n = 10$, implying a s^{-8} behaviour, whereas for $NN \rightarrow NN$ we have $n = 12$, yielding s^{-10} .

There is not a great deal of data on large-momentum-transfer elastic scattering, but what does exist is in reasonable agreement with the counting rules.

However, the Landshoff-type diagrams, Fig. 14.4, lead to a slower decrease with s at fixed θ (Landshoff, 1974). For example, for $NN \rightarrow NN$ the behaviour is s^{-8} . It was argued, however, that the normalization of these contributions would be much smaller than that of the Brodsky–Lepage diagrams (Brodsky and Lepage, 1980). In fact Botts and Sterman (1989) demonstrated that Sudakov suppression is very important for the

Landshoff diagrams and they estimated that for $NN \rightarrow NN$ the naive behaviour is modified to $s^{-9.66}$, quite close to the dimensional counting-rule result s^{-10} .

So, as regards cross-sections, although it has not yet been possible to calculate the hundreds of thousands of Feynman diagrams involved, at least for the broad pattern of decrease with increasing momentum transfer there seems to be agreement between theory and experiment. Moreover, the inclusion of Sudakov effects negates much of the criticism against the premature use of the perturbative results. There has thus been considerable progress in understanding, at a deeper level, the large- p_T dependence.

14.3.3 Summary

Where does all this leave the problem of the analysing power in $pp \rightarrow pp$? At first sight we are no better off than before, since the sophisticated ingredients now included appear to have no effect upon the helicity rule (14.3.2). However, an interesting development was the discovery by Gouset, Pire and Ralston (1996), in the context of meson–meson scattering, that the Landshoff-type diagrams permit wave functions with non-zero L_z , which are not suppressed by $1/s$ as they are in the Brodsky–Lepage hard scattering diagrams. There is some suppression, but it is much milder, $\approx s^{-0.55}$. This would imply that the helicity rule (14.3.2) only becomes valid at extremely large momentum transfer. Unfortunately this discovery does not directly resolve the problem of the proton–proton analysing power, since it turns out that the permitted change in total helicity has to be an *even* number, at least for the meson–meson case studied.

It is hoped, though not yet demonstrated, that this kind of mechanism will lead to the possibility of single helicity-flip in the Landshoff diagrams for $pp \rightarrow pp$. There remains the question of generating a phase difference between the flip and non-flip amplitudes in (14.3.4). The Sudakov factors indeed possess a non-zero phase, but whether there is a significant difference between the phase of ϕ_5 and the non-flip amplitudes is unclear. Our own, perhaps simplistic, guess is that there will be no difference of phase.

It is also possible to generate a single helicity-flip if the nucleon is regarded as a quark–diquark system that includes a component in the wave function corresponding to a spin-1 vector diquark. In this way, Kroll and collaborators (see e.g. Jakob, Kroll, Schürmann and Schweiger, 1993) have been able to obtain, amongst other things, a reasonable description of the Pauli electromagnetic form factor $F_2(Q^2)$ of the proton, which involves a nucleon single helicity-flip matrix element.

Goloskokov and Kroll (1999) have attempted to estimate the analysing power in $pp \rightarrow pp$ using the quark–diquark picture. The helicity non-flip amplitude is modelled phenomenologically so that it corresponds

to what one might expect from multiple pomeron exchange (Section 14.1). The helicity-flip amplitude ϕ_5 is calculated perturbatively using two-gluon exchange diagrams. The proton Fock state contains both scalar and vector diquarks, but to simplify the calculation only the scalar is used in estimating the non-flip vertex in ϕ_5 , and only the vector in the flip vertex.

With all the approximations made, this model is not expected nor tuned to agree with the data, but numerical studies show that it does provide an acceptable, approximately energy-independent, analysing power, which, however, eventually decreases with increasing momentum transfer and finally merges into the Brodsky–Lepage hard scattering result.

The quark–diquark picture is best regarded as a model for higher-twist effects and as such would lead to an analysing power that ultimately decreases like $1/s$ at fixed angle. In the Gousset *et al.* picture, if it can really produce a non-zero analysing power, that too will eventually tend to zero, but probably more slowly than $1/s$.

In either case it seems unavoidable that ultimately QCD demands that $A \rightarrow 0$ as p_T increases. But we have no concrete predictions for A nor for the scale at which the decrease should begin to be seen. Given the exciting experimental possibilities about to open up at the RHIC collider, this is, alas, a most frustrating state of affairs and we can only hope for a major theoretical breakthrough.